Rare Metal Materials and Engineering
Volume 45, Issue 1, January 2016
Online English edition of the Chinese language journal

Available online at www.sciencedirect.com
ScienceDirect

Cite this article as: Rare Metal Materials and Engineering, 2016, 45(1): 0056-0061.

ARTICLE

Structures and Hydrogen Storage Properties of $La_{1-x}Mg_xNi_{4.25}Al_{0.75}$ (x=0.0, 0.1, 0.2, 0.3) Alloys

Lü Lijun[1,3], Cheng Honghui[1,2], Han Xingbo[1], Lei Guanhong[1], Tang Xiaoxing[1], Wang Chengbin[1], Liu Wei [1], Li Xiaolin[1]

[1] Shanghai Institute of Applied Physics, Chinese Academy of Sciences, Shanghai 201800, China; [2] Yangzhou University, Yangzhou 225127, China; [3]University of Chinese Academy of Sciences, Beijing 100049, China

Abstract: $La_{1-x}Mg_xNi_{4.25}Al_{0.75}$ (x=0.0, 0.1, 0.2, 0.3) hydrogen storage alloys were prepared by a three-step induction melting. Their crystal structures and hydrogen storage properties were investigated. Results show that alloys with x=0.0 and 0.1 contain a single $LaNi_4Al$ phase; however, those with x=0.2 and 0.3 are composed of $LaNi_4Al$, (La, Mg)Ni_3 and $AlNi_3$ phases. With x increasing from 0.2 to 0.3, the abundances of the secondary phases and the plateau pressures in the pressure-composition isotherms are lifted significantly. Meanwhile, their hydrogen storage capacities are remarkably reduced. It is found that the alloy with x=0.1 possesses the fastest absorption kinetics compared to the others as well as a good hydrogen capacity and a low plateau pressure.

Key words: RE hydrogen storage alloy; Mg substitution; hydrogen storage property

The importance of hydrogen as a clean energy carrier is being widely accepted during recent years, since more and more people recognize that the combustions of fossil fuels would produce such greenhouse gases as oxides of carbon, nitrogen, sulphur, etc.[1] which are harmful to the environments and economies. Hydrogen is considered as a potentially non-carbon-based and alternatively eco-friendly fuel, which can be generated from clean and renewable sources[2].

For the coming hydrogen economy society, efficient hydrogen storage and delivery are fundamentally important. AB_5-type alloys are preferably used for hydrogen storage. They can reversibly uptake/release hydrogen in ambient conditions. Element substitution has been frequently adopted to improve the ab/de-sorption properties of such alloys[3-6]. As a favorable material, $LaNi_{4.25}Al_{0.75}$ is used in storing tritium in such facilities as the Savannah River Site (SRS) of USA[7]. Since it is liable to be activated, a delivery pressure higher than 200 kPa can be easily achieved by a moderate heating and nearly entire ^{3}He can be captured. So far, $LaNi_{4.25}Al_{0.75}$ alloy as the tritium storage medium has been employed for more than 20 years[8]. Cheng et al.[9] found that the hydrogen absorption kinetics of the unannealed melt-spun (UMS) $LaNi_{4.25}Al_{0.75}$ alloy was improved from that of annealed induction-melt (AIM) one after 1500 cycles. Furthermore, the utilization of melt-spinning technique resulted in a decreased hysteresis of pressure-composition (P-C) isotherms and an improved pulverization resistance.

In recent years, Mg and Mg-Ni-based alloys have been adopted for on-board hydrogen storage materials because of their high capacity[10,11]. In addition, Mg-based hydrides possess some excellent properties such as recyclability, reversibility and heat-resistance[12]. Hence, partial substitution of La by Mg in $LaNi_{4.25}Al_{0.75}$ alloy was expected to improve the ab/de-sorption properties. Moreover, the substitution would decrease the cost of the product because Mg is much cheaper than La. However, little attention was paid on the substitution of La by Mg in $LaNi_{4.25}Al_{0.75}$ alloy at present. Therefore, we would focus on the crystal structures and the

Received date: January 19, 2015
Foundation item: Strategic Priority Research Program of the Chinese Academy of Sciences (XDA02020200); National Natural Science Foundation of China (11475145)
Corresponding author: Cheng Honghui, Ph. D., Associate Professor, College of Mechanical Engineering, Yangzhou University, Yangzhou 225127, P. R. China, Tel: 0086-514-87859737, E-mail: 31834385@qq.com

hydrogen storage properties of $La_{1-x}Mg_xNi_{4.25}Al_{0.75}$($x$=0.0, 0.1, 0.2, 0.3) alloys.

1 Experiment

The $La_{(1-x)}Mg_xNi_{4.25}Al_{0.75}$ alloys were prepared by electro-magnetic induction melting the mixtures of La (99.50%), Ni (99.90%), Al (99.99%) and Mg (99.95%) ingots, using the furnace with a cold crucible under argon atmosphere in the Metallurgical Laboratory of Shanghai University. Because the saturated vapor pressure of magnesium is remarkably high, a three-step melting process was adopted to reduce the loss of Mg. Firstly, $La_{1-x}Ni_{4.25}Al_{0.75}$ alloy was prepared with Al, La and Ni ingots which were placed in crucible from bottom to top. After the preparation, the as-cast ingot of $La_{1-x}Ni_{4.25}Al_{0.75}$ alloy was mechanically pulverized. Secondly, Mg was plunged into the bottom of crucible and covered with $La_{1-x}Ni_{4.25}Al_{0.75}$ pieces to produce $La_{1-x}Mg_xNi_{4.25}Al_{0.75}$ alloy. Afterward, the as-cast $La_{1-x}Mg_xNi_{4.25}Al_{0.75}$ alloy was crushed into pieces and melted again under the same conditions in order to obtain a homogeneous alloy. At last, the as-cast ingots were sealed in quartz tubes under argon atmosphere for annealing. The annealing was conducted in a muffle furnace at 1173 K for 4 h. After that, the samples were slowly cooled down to room temperature. Since magnesium might lose mass by nearly 15% during the whole process as above mentioned, an excessive Mg of 15% was added to compensate the loss.

The chemical composition of the alloys was determined by inductively coupled plasma optical emission spectrometry (ICP-OES，SPECTRO ARCOS SOP type, Germany). About 200 mg powder with uniform composition was weighed for ICP-OES analysis. Three parallel samples were analyzed for each alloy to ensure reproducibility.

The crystal structures of the alloys were determined by an X-ray diffractometer (XRD, Bruker, D8 ADVANCE type, Germany). The X-ray diffractometer worked with the X-ray of Cu Kα and scanned in the 2θ range from 10° to 90° at room temperature. The scanning step size and dwell times per step were 0.02° and 0.15 s, respectively. For the XRD analysis, the alloy samples were mechanically crushed and ground into powders. The Rietveld refinements on the XRD pattern were applied to determine the phase abundances and lattice parameters by the TOPAS software (Bruker).

The hydrogen absorption/desorption *P-C* isotherms of the alloys were measured on a Sieverts apparatus[13] with 99.999% purity hydrogen gas at New Energy Material & Technology Laboratory of Yangzhou University. The samples of about 1g were put into the reaction chamber, evacuated at 373 K for 30 min, and then reacted with 9 MPa hydrogen. After 10 absorption-desorption cycles, the alloys were fully activated. Subsequently, the *P-C* isotherms of the hydrogen absorption/desorption and the hydrogen absorption kinetics curves were measured at 363, 383 and 403 K. In the present paper, $t_{0.9}$ represents the time taken for absorbing 90% of the maximum hydrogen capacity of an alloy. The slope factor S_f was defined as:

$$S_f = \lg \frac{p_{wt\%=0.8}}{p_{wt\%=0.14}} \quad (1)$$

where $p_{wt\%=0.8}$ and $p_{wt\%=0.14}$ are the plateau pressures for a hydrogen storage capacity of 0.8 wt% and 0.14 wt%, respectively.

2 Results and Discussion

2.1 Alloy phases and crystal structures

The comparison of the ICP-OES results with the designed compositions of $La_{1-x}Mg_xNi_{4.25}Al_{0.75}$ alloys in Table 1 reveals that the ICP-OES results agreed well with the designed alloy compositions, with a relative deviation of La, Ni, Al and Mg content of about ±5% for most of the alloy samples.

The XRD patterns in Fig.1 have characterized three phases in the $La_{1-x}Mg_xNi_{4.25}Al_{0.75}$ (x=0.0, 0.1, 0.2, 0.3) alloys, which are $LaNi_4Al$ phase with a $CaCu_5$-type hexagonal structure, $(La,Mg)Ni_3$ phase with a $PuNi_3$-type rhombohedral structure and $AlNi_3$ phase with an $AuCu_3$-type cubic structure. The $LaNi_4Al$ and the $(La,Mg)Ni_3$ are hydrogen absorbable phases, but the $AlNi_3$ is not such kind of phase[14,15]. The Rietveld method was applied in this study for a quantitative phase analysis. As an example, the Rietveld refinement pattern for the alloy with x=0.3 is exhibited in Fig.2. The patterns calculated using the Rietveld method fit well with the patterns obtained by the XRD analysis. For the Rietveld refinements, the structural models for $LaNi_4Al$, $(La,Mg)Ni_3$ and $AlNi_3$ phases were taken from the reported $CaCu_5$[16], $PuNi_3$[17] and $AuCu_3$[18] structures, respectively. Crystal structure characterizations and the evolution of phases abundances for the alloys reveal that the phase structures and abundances of the alloys change with Mg content (Table 2, Fig.3). When x is equal to 0.0 and 0.1, $LaNi_4Al$ is the single phase in the alloys, suggesting that Mg fully dissolves into the alloy with x=0.1. However, when x is increased to 0.2 and 0.3, the $(La,Mg)Ni_3$ and $AlNi_3$ phases appear in the alloys. When x is increased from 0.2 to 0.3, the abundance of the $LaNi_4Al$ phase drops from 67.3 wt% to 52.8 wt%, whereas the abundances of $AlNi_3$ and $(La,Mg)Ni_3$ phases increase from 18.30 wt% to 25.63 wt% and 14.35 wt% to 21.51 wt%, respectively. These structural changes most likely affect the ab/de-sorption properties of the alloys.

Table 2 shows the crystallographic parameters of all phases in the alloys, which coincides well with those published in literatures [14, 19, 20]. The cell volume of the main phase $LaNi_4Al$ slightly decreases with increasing Mg content. While the cell volume of the $(La,Mg)Ni_3$ phase decreases when x is changed from 0.2 to 0.3. The $LaNi_4Al$ phase has a $CaCu_5$-type hexagonal structure. In the present work, the transfer energy

Table 1 Comparison of the designed alloys compositions with the ICP-OES results

Alloy		Element content/wt%			
		La	Mg	Ni	Al
$LaNi_{4.25}Al_{0.75}$	Designed	34.00	–	61.05	4.95
	ICP-OES	33.09±0.03	–	63.28±0.11	4.99±0.01
$La_{0.9}Mg_{0.1}Ni_{4.25}Al_{0.75}$	Designed	31.48	0.61	62.81	5.10
	ICP-OES	32.86±2.07	0.63±0.03	65.45±4.15	5.26±0.25
$La_{0.8}Mg_{0.2}Ni_{4.25}Al_{0.75}$	Designed	28.81	1.26	64.68	5.25
	ICP-OES	27.77±0.20	1.11±0.01	67.40±0.23	5.13±0.08
$La_{0.7}Mg_{0.3}Ni_{4.25}Al_{0.75}$	Designed	25.98	1.95	66.66	5.41
	ICP-OES	25.16±0.0004	1.84±0.01	67.92±0.54	5.28±0.03

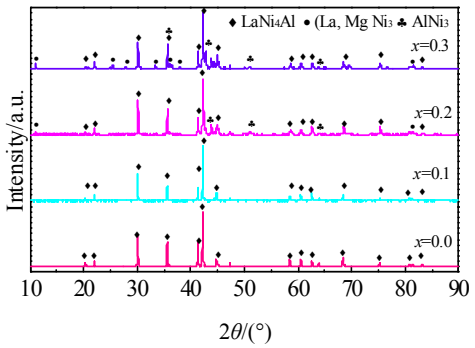

Fig.1 X-ray diffraction patterns of $La_{1-x}Mg_xNi_{4.25}Al_{0.75}$ (x=0.0, 0.1, 0.2, 0.3) alloys

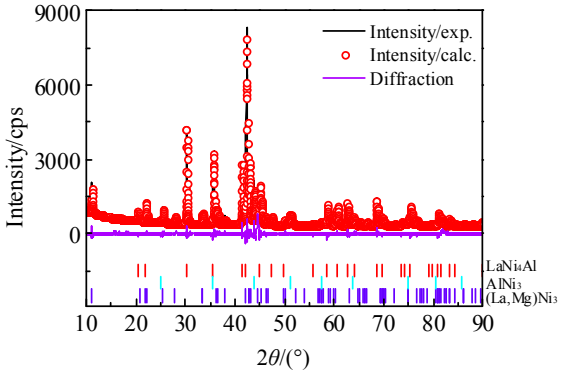

Fig.2 Rietveld refinement of the observed XRD pattern for the alloy with x=0.3

of a Mg atom substituting a La atom in the $CaCu_5$-type phase was calculated to 2.37 eV based on first-principle calculation[21]. This indicates that the Mg atom can substitute La atom in the $LaNi_4Al$ phase. The $PuNi_3$-type (La, Mg)Ni_3 phase is a stacking of $LaNi_5$ and $MgCu_2$ ($MgZn_2$) units along the c-axis. The Mg atom can substitute the La atom only inside the $MgCu_2$ unit (6c site)[22]. The atomic radius of Mg (0.1602 nm) is obviously shorter than that of La (0.1897 nm)[14]. Therefore, the decrease of the cell volumes of the $LaNi_4Al$ and (La, Mg)Ni_3 phases might be due to the substitution of La by Mg. Fig.3 shows the relation between phase abundance and Mg content in the alloys.

2.2 Pressure-composition isotherms

The hydrogen absorption and desorption P-C isotherms of the $La_{1-x}Mg_xNi_{4.25}Al_{0.75}$ (x=0.0, 0.1, 0.2, 0.3) alloys at 363 K are shown in Fig.4. Only one plateau is found in the curves for the alloys with x=0.0 and 0.1, which is attributed to the $LaNi_4Al$ phase. While two plateaus appear in the curves for the alloys with x=0.2 and 0.3. These two regions might be correlated to the $LaNi_4Al$ and (La,Mg)Ni_3 phases, respectively. Zhang L *et al.* reported that the plateau pressure observed for the $LaNi_5$ phase was higher compared to that of the (La,Mg)Ni_3 phase[23], and Zhang X.B. *et al.* showed that the difference between the plateau pressures of AB_5 and AB_3-type compounds is too small to be observed[24]. In the present study, the low plateau region turns narrower and the high plateau region becomes wider as the Mg content increases from 0.2 to 0.3. This change is correlated with the decrease of the $LaNi_4Al$

Table 2 Lattice parameters and phases abundances of the $La_{(1-x)}Mg_xNi_{4.25}Al_{0.75}$ (x=0.0, 0.1, 0.2, 0.3) alloys

Alloy	Phase	Space group	a/nm	c/nm	V/nm^3	Abundance/wt%
$LaNi_{4.25}Al_{0.75}$ R_{wp}=9.03%, S=1.93	$LaNi_4Al$	P6/mmm	0.50504	0.40469	0.08939	100.00
$La_{0.9}Mg_{0.1}Ni_{4.25}Al_{0.75}$ R_{wp}=10.84%, S=2.42	$LaNi_4Al$	P6/mmm	0.50488	0.40455	0.08930	100.00
$La_{0.8}Mg_{0.2}Ni_{4.25}Al_{0.75}$ R_{wp}=8.91%, S=2.03	$LaNi_4Al$	P6/mmm	0.50432	0.40381	0.08895	67.35
	$AlNi_3$	$Pm\bar{3}m$	0.35772	–	0.04577	18.30
	(La,Mg)Ni_3	$R\bar{3}m$	0.49783	2.40887	0.51702	14.35
$La_{0.7}Mg_{0.3}Ni_{4.25}Al_{0.75}$ R_{wp}=9.37%, S=2.22	$LaNi_4Al$	P6/mmm	0.50431	0.40390	0.08891	52.86
	$AlNi_3$	$Pm\bar{3}m$	0.35782	–	0.04581	25.63
	(La,Mg)Ni_3	$R\bar{3}m$	0.49760	2.40996	0.51678	21.51

Note: R_{wp} = weighted pattern factor, S=goodness of fit

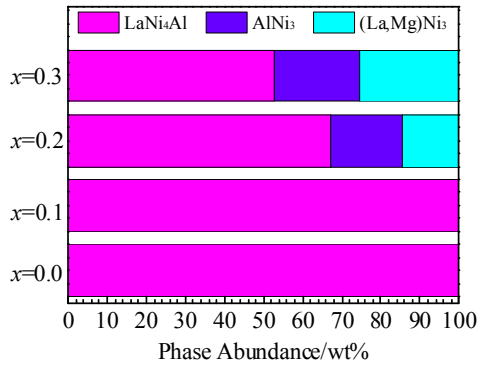

Fig.3 Phase abundances *vs.* Mg content in the alloys

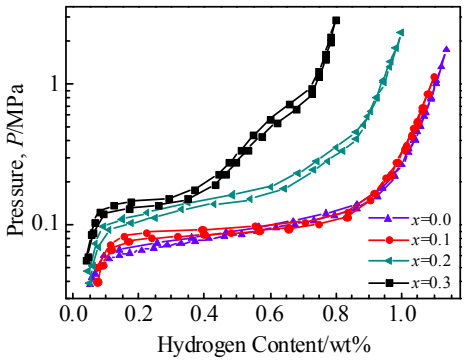

Fig.4 *P-C* isotherms of the $La_{1-x}Mg_xNi_{4.25}Al_{0.75}$ alloys at 363 K

phase abundance and the increase of the $(La,Mg)Ni_3$ phase abundance (Fig.3). Thus, the low and high plateau regions most likely belong to the ab/de-sorption of $LaNi_4Al$ phase and the $(La,Mg)Ni_3$ phase, respectively. Particularly, for the alloy with x=0.3, it is obviously found that the high plateau region is wider than the low plateau region, probably due to the increase of the Mg/La ratio as the Mg content increases in the $(La,Mg)Ni_3$ phase, resulting in an increase of the hydrogen storage capacity [20].

As x increases from 0.2 to 0.3, the hydrogen absorption/desorption plateau pressures increases correspondingly as well. However, only slight increase can be observed for the alloy with x=0.1. These results indicate that the stability of the alloy hydrides decreases as the Mg content in the alloys increases because the increment of the plateau pressure can be regarded as a measure of the stability for the alloy-hydrogen system[25]. The variation of the plateau pressure might be related to the contraction of the unit cell volume of the $LaNi_4Al$ phase and the $(La,Mg)Ni_3$ phase in the alloys (Table 2) because the smaller the unit cell volume, the smaller the interstitial hole size, and hence the larger the strain energy produced when hydrogen atoms occupy interstitial sites [26]. Therefore, the plateau pressure will be higher for a compound with a smaller unit cell volume.

On the other hand, increasing of Mg content from 0.2 to 0.3 results in a degradation of the hydrogen storage capacity from 0.97 wt% to 0.79 wt%. But the hydrogen storage capacity changes very slightly when x is increased from 0.0 to 0.1 (Fig.4). The results of the XRD analyses show that the alloys with x=0.2 and x=0.3 consist of the $LaNi_4Al$, the $(La,Mg)Ni_3$ and the $AlNi_3$ phase (Fig.1). $AlNi_3$ phases is not a hydrogen absorbable phase. The formation enthalpy of $AlNi_3$ is low, which means that $AlNi_3$ is easily generated and very stable[27,28]. The quantitative phase analyses show that the phase abundance of $AlNi_3$ increases from 18.30 wt% to 25.63 wt% as x increases from 0.2 to 0.3 (Table 2). Thus, the degradation of the hydrogen storage capacity may be mainly attributed to the increment of the $AlNi_3$ phase in the alloys. In addition, the decrease of the unit cell volume of the hydrogen absorption phase would lead to the degradation of the hydrogen storage capacity because the hydrogen storage capacity would be geometrically relevant with the free interstitial space and chemically affected by the electronic properties of the lattice atoms surrounding interstitial hydrogen atoms[29].

The plateau slope factor S_f is often used to evaluate the homogeneity of the crystal lattice through distribution of the chemical potential of hydrogen in the hydride[30]. An increasing of S_f usually suggests a poor homogeneity of the alloy. As described above, for the alloys with x=0.2 and 0.3 two plateaus are observed in the *P-C* isotherms, but only one plateau for the alloys with x=0.0 and 0.1 (Fig. 4) can be identified. Thus, the S_f values for the alloys with x=0.2 and 0.3 would be much higher than the corresponding values for the alloys with x = 0.0 and 0.1, implying a lower homogeneity of the crystal lattice for the alloys with x = 0.2 and 0.3 compared to the alloys with x = 0.0 and 0.1. By means of the Eq. (1), the S_f values for the alloys with x=0.0 and x=0.1 were calculated to 0.3 and 0.2, respectively. It indicates that there is no obvious difference between the two alloys. As already mentioned, the magnesium dissolve into a solid solution of the alloy with x=0.1. Therefore, the small amount of Mg in the $LaNi_{4.25}Al_{0.75}$ alloy has little effect on the homogeneity of the alloy.

2.3 Thermodynamic properties

The enthalpies ΔH and the entropies ΔS for the hydrogenation/dehydrogenation of the $La_{1-x}Mg_xNi_{4.25}Al_{0.75}$ alloys were calculated according to the following Van't Hoff equation:

$$\ln\left(\frac{p_{H_2}}{p_0}\right)=\frac{\Delta H}{RT}-\frac{\Delta S}{R} \quad (2)$$

where p_{H_2}, T and R denote the equilibrium hydrogen gas pressure, the sample temperature and the universal gas constant, respectively. The Gibbs free energy ΔG was then calculated using the following equation:

Table 3 Thermodynamic properties of the $La_{1-x}Mg_xNi_{4.25}Al_{0.75}$ (x=0.0, 0.1, 0.2, 0.3) alloys

Alloy	ΔH/kJ·mol^{-1}		ΔS/J·(mol·K)$^{-1}$		ΔG/kJ·mol^{-1} (363 K)		H content/wt%
	Absorption	Desorption	Absorption	Desorption	Absorption	Desorption	
$LaNi_{4.25}Al_{0.75}$	–38.45	38.38	–104.9	104.1	–0.37	0.57	1.12
$La_{0.9}Mg_{0.1}Ni_{4.25}Al_{0.75}$	–38.32	38.34	–105.1	104.5	–0.17	0.39	1.11
$La_{0.8}Mg_{0.2}Ni_{4.25}Al_{0.75}$	–37.81	37.66	–107.2	105.9	1.10	–0.80	0.97
$La_{0.7}Mg_{0.3}Ni_{4.25}Al_{0.75}$	–37.52	37.03	–107.3	105.1	1.43	–1.11	0.79

$$\Delta G = \Delta H - T\Delta S \quad (3)$$

The results of the thermodynamic calculations show that the absolute values of enthalpies decrease with increasing of Mg content, indicating that the hydride stability decrease with increasing of Mg content (Table 3). The results in the table coincide well with the correlation between the increment of the plateau pressure and the increase of the Mg content (Fig.4). The negative values of the Gibbs free energy for the hydrogen absorption (ΔG_a) confirm that the $La_{1-x}Mg_xNi_{4.25}Al_{0.75}$ alloys form stable hydrides and that the hydride stability decreases with increasing of Mg content because the hydrogen absorption reaction is spontaneous in the direction in which the free energy decreases [31].

2.4 Hydrogen absorption kinetics

The hydrogen absorption kinetics of the investigated alloys were assessed by means of isothermal curves. The time taken by the alloys with x=0.0, 0.1, 0.2 and 0.3 to attain 90% of their maximum hydrogenation capacity is 56, 36, 68 and 59 s, respectively (Fig.5). It is found that the hydrogen absorption kinetics of the alloy with x=0.1 is the most significantly improved among these alloys. The capability of the absorption kinetic of an alloy may be correlated to the particle size, the driving force and the hydrogen diffusivity[31]. In order to investigate the powdered features of the alloys, the morphology of the alloys was investigated by scanning electron microscope(SEM) after 15 hydrogen absorption/ desorption cycles (Fig.6). The SEM images show that there is no obvious variation in particle size among the different alloys. Previous research has suggested that the lower the absorption plateau, the greater the driving force for hydriding at the same initial pressure, and hence the absorption kinetics will be fast[32]. The structure of an alloy is better-ordered and its hydrogen diffusivity is faster[33]. As discussed above, the alloys with x=0.0 and 0.1 show a lower absorption plateau and a better homogeneity of the crystal lattice than those with x=0.2 and 0.3. Therefore, the enhanced hydrogen absorption kinetics observed for the alloys with x = 0.0 and 0.1 might be attributed to the greater driving force and hydrogen diffusivity.

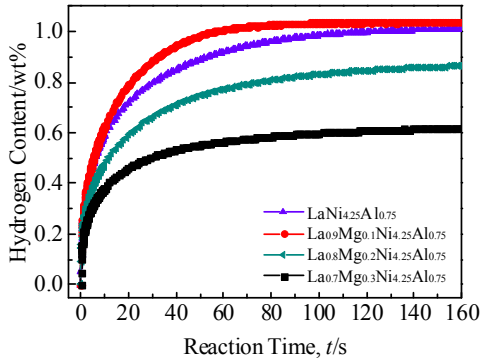

Fig.5 Hydrogen absorption of the $La_{1-x}Mg_xNi_{4.25}Al_{0.75}$ alloys at 363 K

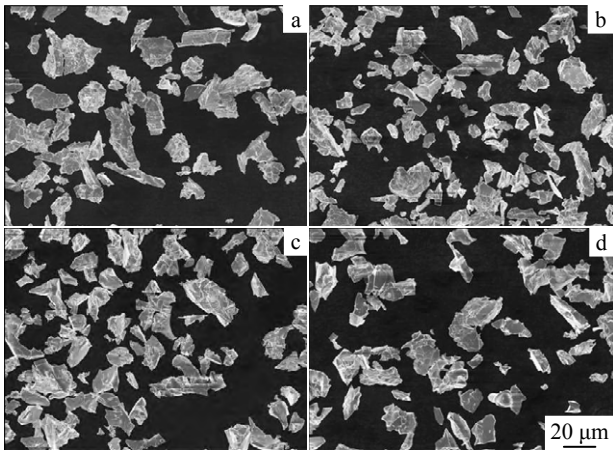

Fig.6 SEM images of the alloys after 15 hydrogen absorption/ desorption cycles: (a) $LaNi_{4.25}Al_{0.75}$, (b) $La_{0.9}Mg_{0.1}Ni_{4.25}Al_{0.75}$, (c) $La_{0.8}Mg_{0.2}Ni_{4.25}Al_{0.75}$, and (d) $La_{0.7}Mg_{0.3}Ni_{4.25}Al_{0.75}$

3 Conclusions

1) The $La_{1-x}Mg_xNi_{4.25}Al_{0.75}$ (x=0.0, 0.1, 0.2, 0.3) alloys show a single phase with a $CaCu_5$-type structure for x=0.0 and 0.1. For x=0.2 and 0.3, however, the presence of secondary phases with a $PuNi_3$-type and an $AuCu_3$-type structures can be identified, and the abundances of the secondary phases increase with increasing of Mg content.

2) With the increase of Mg content from 0.2 to 0.3, the plateau pressure of the alloy increases correspondingly. At the same time, their hydrogen storage capacity decreases from 0.97 wt% to 0.79 wt%, which can be attributed to the increase of the $AlNi_3$ phase abundance in the alloy.

3) The alloy with x=0.1 possesses the fastest absorption kinetics among these alloys, and its plateau pressure and hydrogen capacity are almost the same as those of $LaNi_{4.25}Al_{0.75}$ alloy.

Acknowledgement: The authors are grateful to Prof. Zhong Yunbo

and Ph. D. student Fan Lijun at Metallurgical Laboratory of Shanghai University for alloy preparation.

References

1 Hübert T, Boon-Brett L, Black G *et al*. *Sensors and Actuators B: Chemical*[J], 2011, 157: 329
2 Dutta S. *Journal of Industrial and Engineering Chemistry*[J], 2014, 20: 1148
3 Wang D H, Wu Y J, Yan R X *et al*. *Rare Metal Materials and Engineering*[J], 2008, 37(1): 45 (in Chinese)
4 Jin H J, Zhang J L, Meng X H *et al*. *Rare Metal Materials and Engineering*[J], 2008, 37(5): 803 (in Chinese)
5 Zhang Y H, Li B W, Ren H P *et al*. *Rare Metal Materials and Engineering*[J], 2010, 39(8): 1317 (in Chinese)
6 Zhang Y H, Ren H P, Qi Y *et al*. *Rare Metal Materials and Engineering*[J], 2013, 42(1): 1 (in Chinese)
7 Shanahan K L, Hölder J S, Bell D R *et al*. *Journal of Alloys and Compounds*[J], 2003, 356-357: 382
8 Wang W D, Long X G, Cheng G J *et al*. *Journal of Alloys and Compounds*[J], 2007, 441: 359
9 Cheng H H, Yang H G, Li S L *et al*. *Journal of Alloys and Compounds*[J], 2008, 458: 330
10 Grochala W, Edwards P P. *Chemical Reviews*[J], 2004, 104: 1283
11 Zhu M, Wang H, Ouyang L Z *et al*. *HTM 2004 Hydrogen Treatment of Materials*[J], 2006, 31: 251
12 Sakintuna B, Lamari-Darkrim F, Hirscher M. *International Journal of Hydrogen Energy*[J], 2007, 32: 1121
13 Cheng H H, Li W B, Chen W *et al*. *International Journal of Hydrogen Energy*[J], 2014, 39: 13 596
14 Denys R V,Yartys V A. *Journal of Alloys and Compounds*[J], 2011, 509: 540
15 Zhang R J, Lu M Q, Cao D L *et al*. *Journal of Rare Metals*[J], 2004: 678 (in Chinese)
16 Nakamura H, Nakamura Y, Fujitani S *et al*. *Journal of Alloys and Compounds*[J], 1997, 252: 83
17 Kadir K, Sakai T, Uehara I. *Journal of Alloys and Compounds*[J], 1997, 257: 115
18 Rao P V M, Suryanarayana S V, Murthy K S *et al*. *Journal of Physics: Condensed Matter*[J], 1989, 1(32): 5357
19 Cao D L, Chen D M, Liu Y *et al*. *Transactions of Nonferrous Metals Society of China*[J], 2011, 21(3): 517
20 Liao B, Lei Y Q, Lu G L *et al*. *Journal of Alloys and Compounds*[J], 2003, 356: 746
21 Wang S Y, Wang C Y, Sun J H *et al*. *Physical Review B*[J], 2001, 65: 35 101
22 Liu Y F, Cao Y H, Huang L *et al*. *Journal of Alloys and Compounds*[J], 2011, 509: 675
23 Zhang L, Han S, Li Y *et al*. *International Journal of Hydrogen Energy*[J], 2013, 38: 10 431
24 Zhang X B, Sun D Z, Yin W Y *et al*. *Electrochimica Acta*[J], 2005, 50: 3407
25 Li S L, Wang P, Chen W *et al*. *International Journal of Hydrogen Energy*[J], 2010, 35: 12 391
26 Li S L, Wang P, Chen W *et al*. *International Journal of Hydrogen Energy*[J], 2010, 35: 3537
27 Cheng H H. *Thesis for Doctorate*[D]. Beijing: University of Chinese Academy of Science, 2007
28 Shi D M, Wen B, Melnik R *et al*. *Journal of Solid State Chemistry*[J], 2009, 182: 2664
29 Ye H, Zhang H, Cheng J X *et al*. *Journal of Alloys and Compounds*[J], 2000, 308: 163
30 Nakamura Y, Sato K, Fujitani S *et al*. *Journal of Alloys and Compounds*[J], 1998, 267: 205
31 Li S L, Wang P, Chen W *et al*. *Journal of Alloys and Compounds*[J], 2009, 485: 867
32 Li S L, Cheng H H, Deng X X *et al*. *Journal of Alloys and Compounds*[J], 2008, 460: 186
33 Chou K C, Xu K D. *Intermetallics*[J], 2007, 15: 767

$La_{1-x}Mg_xNi_{4.25}Al_{0.75}$ (x=0.0, 0.1, 0.2, 0.3) 合金的结构与储氢性能

吕丽君[1,3]，程宏辉[1,2]，韩兴博[1]，雷冠虹[1]，唐晓星[1]，王呈斌[1]，刘　卫[1]，李晓林[1]

(1. 中国科学院上海应用物理研究所，上海 201800)

(2. 扬州大学，江苏 扬州 225127)

(3. 中国科学院大学，北京 100049)

摘　要：采用三步感应熔炼法制备了 $La_{1-x}Mg_xNi_{4.25}Al_{0.75}$ (x=0.0，0.1，0.2，0.3) 储氢合金，研究了该系列合金的晶体结构和储氢性能。结果表明，当 x 为 0.0 和 0.1 时，合金由单一的 $LaNi_4Al$ 相组成；而 x 为 0.2 和 0.3 时，合金由 $LaNi_4Al$ 相, $(La,Mg)Ni_3$ 相和 $AlNi_3$ 相构成。随着 Mg 含量 x 从 0.2 增至 0.3 时，合金的第二相丰度和吸/放氢平衡压明显升高，同时储氢容量减小。研究发现，当 Mg 添加量 x=0.1 时，合金除具有良好的储氢容量和低平台压外，其吸氢动力学性能更好。

关键词：稀土储氢合金；Mg 替代；储氢性能

作者简介：吕丽君, 女, 1988 年生, 博士生, 中国科学院上海应用物理研究所, 上海 201800, 电话：021-39194770, E-mail: lvlijun@sinap.ac.cn